NASA Technical Memorandum 78980

FRICTION AND WEAR OF SINGLE-CRYSTAL MANGANESE-ZINC FERRITE

Kazuhisa Miyoshi and Donald H. Buckley
Lewis Research Center
Cleveland, Ohio

TECHNICAL PAPER to be presented at the
International Conference on Wear of Materials
cosponsored by ASME, ASLE, ASM, ASTM-62, SAE, SME,
Amer. Chem. Soc., AIME, and APS
Dearborn, Michigan, April 16-18, 1979

FRICTION AND WEAR OF SINGLE-CRYSTAL MANGANESE-ZINC FERRITE

by Kazuhisa Miyoshi and Donald H. Buckley
NASA Lewis Research Center
Cleveland, Ohio 44135

ABSTRACT

Sliding friction experiments were conducted with single-crystal manganese-zinc ferrite in contact with itself and with transition metals. Results indicate mating highest atomic density directions ((110)) on matched crystallographic planes exhibit the lowest coefficient of friction indicating that direction is important in the friction behavior of ferrite. Matched parallel high atomic density planes and crystallographic directions at the interface exhibit low coefficients of friction. The coefficients of friction for ferrite in contact with various metals are related to the relative chemical activity of these metals. The more active the metal, the higher the coefficient of friction. Cracking and the formation of hexagon- and rectangular-shaped platelet wear debris due to cleavages of {110} planes are observed on the ferrite surfaces as a result of sliding.

INTRODUCTION

Manganese-zinc ferrite is becoming increasingly important as a typical magnetic material used for highly developed magnetic recording devices, e.g., video tape recorders. Most of the high recording-density devices are the system in which the recording and playback are conducted with a magnetic head in sliding contact with a magnetic tape. Therefore, the magnetic head and tape are required to have good wear resistance and low friction.

The manganese-zinc ferrite is used practically in both single-crystal and polycrystalline form. The uses of single-crystal and polycrystalline hot-pressed manganese-zinc ferrite in magnetic heads for industrial and home-use video and audio tape recorders has played a role in the explosion of magnetic recording technology. The life and wear resistance of the ferrite magnetic heads are 5 to 10 times than are those for various metal heads.

The medium actually used in magnetic recording can be classified as metallic or nonmetallic. It is also possible to classify the various media by their geometry: wire, tape, and rigid. The media for high recording density have been in tape form. γ-Fe_2O_3 and Cr_2O_3 tapes have usually been used as tape materials, but iron-base alloy tapes have also been recently developed and they are attracting attention.

The friction and wear properties of magnetic ceramic materials in contact with metals and ceramics under a variety of exacting environmental conditions are, however, not fully understood. Very little experimental work has been done, for example, with manganese-zinc ferrite, a commonly used magnetic ceramic (1,2). Fundamental studies on the friction and wear behavior of magnetic ceramic materials in contact with metals and ceramics should commence with clean surfaces. Such surfaces can be obtained and maintained in a vacuum environment. Once the behavior of clean surfaces is understood, the effect of environmental constituents on friction and wear can be identified. Thus, the friction and wear behavior of magnetic ceramic materials in high vacuum is important. In addition, the knowledge gained in such studies may assist in achieving a better understanding of the friction and wear properties of brittle materials.

The present investigation was conducted to examine the friction and wear behavior of single-crystal manganese-zinc ferrite {100}, {110}, {111}, or {211} surfaces sliding against themselves and various transition metals. All experiments were conducted with loads of 0.05 to 0.5 N (5 to 50 g), at a sliding velocity of 3 mm/min with a total sliding distance of 2.5 millimeters in a vacuum of 10^{-8} N/m^2 and at room temperature.

MATERIALS

The single-crystal manganese-zinc ferrite as-grown platelets were 99.9-percent-pure oxide. The composition and hardness data on manganese-zinc ferrite are presented in table I. The spinel crystal structure of manganese-zinc ferrite is illustrated in figure 1. The crystal is that of spinels in which the oxygen ions are in a nearly close-packed cubic array. In the unit cell, which contains 32 oxygen ions, there are 32 octahedral sites and 64 tetrahedral sites; of those, 16 of the octahedral sites are filled with divalent (Mn^{2+}, Zn^{2+}, Fe^{2+}) and trivalent (Fe^{3+}) ions which are equally divided, and 8 of the tetrahedral sites are filled with trivalent ions (Fe^{3+})(3,4).

All of the metals were polycrystalline. The titanium was 99.97 percent pure, and all the other metals were 99.99 percent pure, as presented in table II.

EXPERIMENTAL APPARATUS AND PROCEDURE

Apparatus

The experiments were conducted in a vacuum chamber. The vacuum chamber contains a system capable of measuring adhesion, load and friction as well as providing Auger surface analysis. The mechanism for applying load and measuring adhesion and friction is shown in figure 2. A gimbal-mounted beam projected into the vacuum system. The beam contained two flats

machined normal to each other with strain gages mounted thereon. The end of the rod contained the single-crystal manganese-zinc ferrite pin specimen (rider). The load was applied by moving the beam toward the flat plate (disk) and was measured by the strain gage. The tangential motion of the pin (rider) along the flat plate (disk) was accomplished through the gimbal assembly. Under an applied load, the friction force was sensed by the strain gage normal to that used to measure the applied load. Pin (rider) sliding was as indicated in figure 2. The vacuum apparatus in which the components of figure 2 were contained also had an Auger spectrometer. The electron beam of both could be focused on any flat-plate (disk) site desired. This was accomplished with a flat-plate (disk) manipulation device. The vacuum system was a conventional vacsorb and ion-pumped system capable of readily achieving pressures of 1.33×10^{-8} N/m^2 (10^{-10} torr) as measured by a nude ionization gage within the specimen chamber. Sublimation pumping was also used to more rapidly achieve the pressure desired.

Specimen Preparation

The surfaces of the single-crystal manganese-zinc ferrite and the polycrystalline metal pin specimens (riders) were hemispherical and were polished with approximately 3-μm-diameter diamond powder and then 1-μm-diameter aluminum oxide (Al_2O_3) powder. The orientation of the ferrite riders are shown in figure 3(a) and are within $\pm 2^\circ$ of the indicated orientation. For the {100}-orientation at the interface, the {100} plane of the rider specimen was oriented such that it was nearly parallel to the sliding interface. For the {110}- and {111}-orientations, rider specimens were also oriented as indicated in figure 3(a). The radius of curvature of the ferrite and metal riders was 0.79 mm (1/32 in.).

The surfaces of disk specimen of the single-crystal manganese-zinc ferrite were also polished with 3-μm-diameter diamond powder and then 1-μm-diameter aluminum oxide powder. The orientations of the ferrite disks are shown in figure 3(b) and are within $\pm 1^\circ$ or less of the indicated orientation. For {100}-orientation at the interface, the {100} plane of the disk specimen was oriented such that it was nearly parallel to the sliding interface. For the other, the {110}-, {111}-, and {211}-orientations, disk specimens were also oriented as indicated in figure 3(b). The method used for determining the orientation of single-crystal was the back-reflection Laue technique.

Both disks and riders of ferrite were also chemically polished with hydrochloric acid at $50^\circ \pm 1^\circ$ C for 2 minutes after mechanically polishing as mentioned above in order to establish the effect of the deformed layer of the surface on friction behavior.

Procedure

The surfaces of the disk and rider specimens were rinsed with absolute ethyl alcohol before the experiment.

For the experiments in vacuum, the specimens were placed in the vacuum chamber and the system evacuated and baked out to achieve a pressure of 1.33×10^{-8} N/m^2 (10^{-10} torr). When this vacuum was achieved, argon gas was bled back into the vacuum chamber to a pressure of 1.3 N/m^2. A 1000-volt, direct-current potential was applied and the specimens (disk and rider) were argon sputter bombarded for 30 minutes. The vacuum chamber was then reevacuated and Auger spectra of the disk surface were obtained to determine the degree of surface cleanliness. When disk surface was clean, friction experiments were conducted.

Loads of 0.05 to 0.5 N were applied to pin (rider)-disk contact by deflecting the beam of figure 2. Both load and friction force were continuously monitored during a friction experiment. Sliding velocity was 3 millimeters per minute with a total sliding distance of 2.5 millimeters. All friction experiments were conducted with the system reevacuated to a pressure of 10^{-8} N/m^2.

RESULTS AND DISCUSSION

Auger Analysis of Manganese-Zinc Ferrite Surfaces

Auger spectra of the as-received single-crystal manganese-zinc ferrite surface were obtained before and after sputter cleaning. The spectra obtained before sputter cleaning revealed that, in addition to the oxygen and iron, a carbon contamination peak was evident (5). An Auger spectrum for ferrite {110} surface after sputter cleaning is shown in figure 4. The carbon contamination peak has completely disappeared from the spectrum. In addition to oxygen and iron, Auger peaks indicate small amounts of manganese, zinc on the surface. If the oxygen peak was compared to that of the iron peak on the {100}, {110}, {111}, and {211} surfaces, the oxygen to iron peak height ratio indicated that the surface accommodation for oxygen was in the order for the various planes of, {110} > {211} > {111} > {100}.

Friction and Wear Behavior of Ferrite in Contact with Itself

Deformation effects of mechanical polishing or friction. Sliding friction experiments were conducted with an etched surface of {100} rider in contact with both etched and mechanically polished surfaces of {110} disk specimens in the ⟨110⟩ sliding direction. An examination with high-energy reflection electron diffraction revealed a single-crystal spot pattern or Kikuchi lines, which indicates perfection of the crystal structure, from the etched {110} disk surfaces. Debye ring (mostly diffuse) pattern generally appeared on the mechanically polished surface. This pattern might indicate a oriented layer or texture of the mechanically polished surface.

Friction force traces of both etched and mechanically polished surfaces of ferrite in contact with itself are generally characterized by marked stick-slip behavior. This type of friction is expected where strong adhesion occurs at the interface.

Figure 5 presents the coefficients of friction, calculated from maximum peaks in the friction traces, as a function of angle between {100} plane of the rider and {110} sliding surface of the disk. The {110} disk specimen was inclined at various angles with respect to the mating rider. The disk were turned relative to the rider on an axis in the {110} direction. Sliding was in the ⟨110⟩ direction on both rider and disk. The data of figure 5 indicate that the coefficients of friction for both etched and mechanically polished surfaces are not significantly different and the trend of the data are similar. Thus, the succeeding experiments were conducted with mechanically polished ferrite surfaces.

Influence of crystallographic plane on friction. Sliding friction experiments were conducted with the {100}, {110}, and {111} planes of riders in contact

with those planes of disks. The disks were inclined at various angles with respect to the mating riders. All disks were turned relative to the rider on an axis in the ⟨110⟩ direction of the rider to achieve the desired orientation. All sliding was in the ⟨110⟩ direction on both riders and disks. The data of figure 6 indicate that the coefficient of friction is lowest with the {100}, {110}, and {111} plane of the rider parallel to the interface, that is, at an angle of zero to the sliding mating surface. This is due to the interface of higher atomic density achieved with parallel planes than with surfaces inclined at various angles. This is consistent with earlier studies (6,7). The coefficients of friction reported herein were obtained from the results of measurements of three to five friction traces. The deviation in friction with repeated experiment was ±10 percent of that indicated in the figure.

The coefficients of friction for three crystallographic planes of ferrite, {100}, {110}, and {111}, in contact with themselves were not significantly different. It might be anticipated from these results that the atomic density for {100}, {110}, and {111} planes would be nearly the same because the distribution of the cations in the available sites is very complicated in a spinel crystal, as shown in figure 1.

Sliding friction experiments were also conducted with the {110} plane of ferrite riders in contact with {100}, {111}, and {211} planes of the disks, respectively. The disks were inclined at various angles with respect to the mating riders. Disks were turned around on an axis in the ⟨110⟩ direction of rider, and sliding was in the ⟨110⟩ direction on both rider and disks. The data of figure 7 reveal that the coefficients of friction for three mated dissimilar crystallographic planes, {110} on {100}, {110} on {111}, and {110} on {211} were nearly the same as those for matched crystallographic planes in contacts in figure 6. However, in figure 7, as anticipated, there is an absence of a friction minimum at an angle of zero to the interface.

Influence of crystallographic direction on friction. It might be anticipated from preceding results shown in figure 5 that the mating crystallographic directions of both rider and disk would give rise to a significant difference in the coefficient of friction. Therefore, the influence of crystallographic direction on friction is a matter of interest.

The coefficients of friction for three matched crystallographic planes in same and dissimilar directions are plotted in figure 8. In the experiments herein, the {110} rider slid on the flat surfaces of the {110}, {111}, and {211} planes in the same and dissimilar crystallographic directions to that of the rider. Sliding in the same direction was in the ⟨110⟩ directions on both the riders and disks, as already shown in figures 6 and 7. The sliding of dissimilar direction was in the ⟨110⟩ direction on the rider, and in the ⟨100⟩ direction on the {110} surface of the disk, ⟨211⟩ on {111} disk and ⟨111⟩ on {211} disk. The differences in coefficients of friction with respect to the mating crystallographic directions are significant, as expected. The coefficients of friction for the three matched crystallographic planes in the dissimilar directions are generally higher than those in the same directions and vary according to the indication of the surface of the disk at various angles.

The coefficient of friction is lowest with {110} plane of rider parallel to the interface, namely at the angle of zero to the sliding mating surface. Thus, mating highest atomic density directions on matched crystallographic planes exhibits the lowest coefficient of friction, and mating higher atomic density planes may also exhibit lower coefficient of friction. These results indicate that mating the crystallographic direction can specially play a significant role in friction behavior of ferrite. Sliding along the direction, which is most closely packed, may minimize the adhesive friction.

Anisotropic wear behavior. Following the single pass experiments in the former section, multipass experiments were conducted to establish steady state conditions. When repeated passes were made of the ferrite rider over the same ferrite at a load of 0.2 N (20 g), the coefficient of friction was constant or slightly increased with the number of passes. The friction traces under repeated passes were characcerized by stick-slip behavior over the entire number of passes.

Anisotropy of wear behavior of the ferrite surface is observed with (1) cracking and (2) the wear debris generated by fracture.

(1) Cracking - The sliding of ferrite results in surface cracks along the {110} planes. Figures 9(a) and (b) show scanning electron micrographs of the rider wear scar and the disk wear track as a result of 5 passes of the rider on the same disk surface. The {110} of the rider and {211} of the disk were parallel to the sliding interface. Small cracks, which zig-zag along cleavage planes of the {110}, are clearly observed on both rider and disk. Such small cracks propagated along cleavage planes of {110} and were observed with the surfaces of other riders and disks, (e.g., the {100} and {111}.).

Figure 10 contains a scanning electron micrograph of the cracks propagated along the {110} planes and a fracture pit on the rider as a result of 20 passes over the ferrite {110} surface. The formation of a fracture pit is primarily due to cleavage-cracking along {110} planes and sub-surface cracking along {110} planes. The smooth surface at the bottom of fracture pit is due to sub-surface cleavage of the {110} planes. Thus, the fracture behavior of the ferrite crystal during sliding, is significantly dependent on the cleavage systems of {110} planes.

(2) Wear debris - It might be anticipated from the preceding figures 9 and 10 that the wear debris would be some polygon-shaped platelet, where the sides are produced by cleavage cracking. Two types of wear debris are observed, as shown in figures 11(a) to (c). One type is characterized by consisting of hexagon-shaped particles. Figures 11(a) and (b) reveal the wear particles of the rider transferred to the surface of the disk. Both {110} planes of the rider and the disk were parallel to the sliding interface. The wear particles have a nearly full hexagon-shape as well as a partial hexagon shape, and are flat. The formation of platelet hexagon-shape is due to cleavage of {110} planes, where the values of angles between different {110} planes on a {110} sliding surface are 60° or common multiples thereof. The platelet flat is due to the cleavage of {110} planes in the bulk, parallel to the sliding interface.

The second type of wear debris is rectangular in shape. Figure 11(c) reveals a dislodged wear particle of the disk, with its fracture surface exposed. The {100} plane of the disk was parallel to the sliding interface. The wear particle has a nearly rectangular-shape. The exposed fracture surfaces of the wear debris have cleavage steps. The risers of the steps may be {110} planes. The ledges of steps are very

smooth and the formation of the ledge may be due to sub-surface cracking of {110} planes in the disk. The formation of a rectangular-shaped platelet is also due to cleavage of {110} planes, where the values of angle between different {110} planes on the {100} sliding surface are 90° or common multiples thereof. Thus, hexagon- and rectangular-shaped wear debris may be produced by cleavage systems of {110} planes under high adhesive and shearing forces. This is also consistent with an earlier study (8). In that study, sliding friction experiments were conducted with single-crystal, hexagonal silicon carbide sliding against itself and against titanium. The results indicated hexagonal-shaped fracture of silicon carbide and the formation of platelet hexagon-shaped wear debris of silicon carbide due to primary cleavages of both prismatic and basal planes when silicon carbide was sliding against itself.

Friction and Wear Behavior of Ferrite in Contact with Various Metals

Effect of metal activity on friction. The relative chemical activity of the transition metals (metals with partially filled d shells) as a group can be ascertained from their percent d bond character after Pauling (9). The friction properties of metal-metal contacts and metal-ceramic contacts have been shown to be related to this character (10,11). The greater the percent of d bond character, the less active is the metal. The more active the metal, the higher the coefficient of friction.

Sliding friction experiments were conducted with ferrite in contact with a number of transition metals. The friction traces with metal-ferrite couples are generally characterized by smoothly fluctuating behavior with no evidence of stick-slip, but the traces under higher loads are characterized by stick-slip behavior. With the chemically more active metal titanium, more marked stick-slip behavior appears at a load of 0.2 N (20 g). With the chemically less active metal rhodium, stick-slip behavior appears under higher loads of 0.35 N or more. The coefficients of friction for various metals sliding on ferrite were unaffected by load in the range of 0.05 N to 0.5 N.

The coefficients of friction for various metals with ferrite are presented in figure 12 as a function of the d bond character of the transition metal. There appears to be good agreement between friction and chemical activity of the transition metals. Titanium, having strong chemical affinity for iron and oxygen in ferrite, exhibits considerably higher friction in contact with ferrite than does rhodium, which has a lesser affinity for these same two elements.

Wear behavior. Examinations of the wear track on ferrite surfaces after sliding with metals revealed occasional evidence of fracture in ferrite. Figure 13 is scanning electron micrographs of wear tracks on ferrite. In figure 13, three types of cracking in the wear track are observed. One type is characterized by a small crack propagating perpendicular to the sliding direction. The second type is a crack propagating at an inclination of about 45° to the sliding direction, that is, along cleavage planes of {110}. The third type obtained is a crack propagating parallel to the sliding direction, that is, also along the cleavage planes of {110}. Thus, the cracking of ferrite in sliding contact with metal is also significantly dependent on the cleavage system of {110} planes as well as ferrite-ferrite contacts as already discussed in the former section.

The three types of cracking were observed with single-crystal manganese-zinc ferrite in sliding contact with spherical diamond riders in nitrogen at atmospheric pressure (1) and with single-crystal silicon carbide in sliding contact with spherical and conical diamond riders in argon at atmospheric pressure (12). Under such conditions, sliding occured at the interface and friction primarily involved shearing at the interface and plowing (plastic deformation) in the single-crystal manganese-zinc ferrite and silicon carbide. It is of interest that similar cracking occurs in nominally brittle materials regardless of marked differences in friction behavior and environments.

The fracturing and formation of wear debris of ferrite in contact with metal are the result of cracks being generated, propagating and then intersecting. Figure 14 presents a scanning electron micrograph and an X-ray map of a wear scar of metal rider generated by five passes sliding on ferrite disk. The wear scar on metal rider may generally contain small wear debris particles generated by the fracture of the ferrite surface, as shown in figure 14. Titanium, having strong chemical activity, exhibited considerably more wear debris particles of ferrite transferred (embedded) to metal surface than did rhodium or iron, having lesser chemical activity. Thus, wear debris of ferrite may be produced by cleavage cracking and be transferred to or embedded in the metal during sliding.

Lastly, all examinations of the wear track on ferrite surfaces after sliding with metals revealed evidence of metal transfer to ferrite. The transfer and wear behavior of various transition metals was similar to those in sliding friction experiments conducted with single-crystal silicon carbide sliding against various transition metals in vacuum (11); that is, the more active the metal, the greater the transfer to ferrite and the rougher the wear scar on the surface of the metal.

CONCLUSIONS

As a result of the sliding friction experiments conducted in this investigation with single-crystal manganese-zinc ferrite {100}, {110}, {111}, and {211} surfaces in sliding contact with themselves and with various metals, the following conclusions are drawn:

1. Mating highest atomic density (most closely packed) directions (⟨110⟩) on matched crystallographic planes exhibit the lowest coefficient of friction indicating that direction is important in the friction behavior of ferrite.

2. Matched parallel high atomic density planes and crystallographic directions at the interface exhibit low coefficients of friction. Mating dissimilar crystallographic planes, however, does not give a significant difference in friction from that observed with matched planes.

3. The coefficients of friction for ferrite in contact with various metals are related to the relative chemical activity of these metals. The more active the metal, the higher the coefficient of friction.

4. Cracking, and the formation of hexagon- and rectangular-shaped platelet wear debris are observed on the ferrite surfaces as a result of sliding. The cracking and formation of such wear debris particles are primarily due to cleavage of {110} planes on the surface and in the bulk of ferrite.

5. All metals examined transferred to the surfaces of ferrite in sliding.

ACKNOWLEDGEMENT

The authors wish to thank Prof. Kyuichiro Tanaka of Kanazawa University in Japan for supplying the materials.

REFERENCES

1. Tanaka, K.; et al: Friction and Deformation of Mn-Zn Ferrite Single Crystals. Proceedings of the JSLE/ASLE International Lubrication Conference, T. Sakurai, ed., Elsevier Scientific Publishing Co., 1976, pp. 58-66.

2. Van Groenou, A. Broese; Maan, N.; and Veldkamp, J. D. B.: Scratching Experiments on Various Ceramic Materials. Philips Res. Rep., vol. 30, no. 5, Oct. 1975, pp. 320-359.

3. Von Hippel, Arthur R.: Dielectrics and Waves. John Wiley & Sons, Inc., 1954, pp. 219-228.

4. Kingery, W. D.; Bowen, H. K.; and Uhlmann, D. R.: Introduction to Ceramics. Second ed. John Wiley & Sons, Inc., 1976, pp. 25-88 and pp. 975-1015.

5. Miyoshi, K.; and Buckley, Donald H.: Friction and Wear of Single-Crystal and Polycrystalline Manganese-Zinc Ferrite in Contact with Various Metals. NASA TP-1059, 1977.

6. Buckley, Donald H.: The Influence of the Atomic Nature of Crystalline Materials on Friction. Trans. ASLE, vol. 11, 1968, pp. 89-100.

7. Johnson, R. L.; and Buckley, Donald H.: Lubrication and Wear Fundamentals for High-Vacuum Applications. Proc. Inst. Mech. Eng., (London), vol. 182, pt. 3A, 1967-68, pp. 479-490.

8. Miyoshi, K.; and Buckley, D. H.: Friction and Fracture of Single-Crystal Silicon Carbide in Contact with Itself and Titanium. Trans. ASLE, in process.

9. Pauling, L.: A Resonating-Valence-Bond Theory of Metals and Intermetallic Compounds. Proc. Roy. Soc. (London), Ser. A, vol. 196, no. 1046, Apr. 7, 1949, pp. 343-362.

10. Buckley, D. H.: The Metal- to Metal Interface and Its Effect on Adhesion and Friction. J. Colloid Interface Sci., vol. 58, no. 1, Jan. 1977, pp. 36-53.

11. Miyoshi, K.; and Buckley, D. H.: Friction and Wear Behavior of Single-Crystal Silicon Carbide in Sliding Contact with Various Metals. Trans. ASLE, in process.

12. Miyoshi, K.; Buckley, D. H.: Friction, Deformation and Fracture of Single-Crystal Silicon Carbide, Trans. ASLE, in process.

TABLE I. - COMPOSITION AND HARDNESS DATA

ON MANGANESE-ZINC FERRITE

	Composition, wt %							
	Fe_2O_3, 71.6			MnO, 17.3		ZnO, 11.1		
Surface	(100)	(100)	(110)	(110)	(111)	(111)	(211)	(211)
Direction	[001]	[011]	[001]	$[\bar{1}10]$	$[11\bar{2}]$	$[1\bar{1}0]$	$[\bar{1}11]$	$[0\bar{1}1]$
Knoop hardness[a]	630	560	630	560	580	600	550	580
Vickers hardness[b]	630	630	645	645	590	590	650	650

[a]Knoop hardness measuring load was 300 grams.

[b]Vickers hardness measuring load was 50 grams.

TABLE II. - CRYSTAL STRUCTURE AND

PURITY OF VARIOUS METALS

Metal	Crystal structure	Purity, percent
W	Body-centered cubic	99.99
Fe	Body-centered cubic	99.99
Ni	Face-centered cubic	99.99
Rh	Face-centered cubic	99.99
Ti	Close-packed hexagonal	99.97
Co	Close-packed hexagonal	99.99

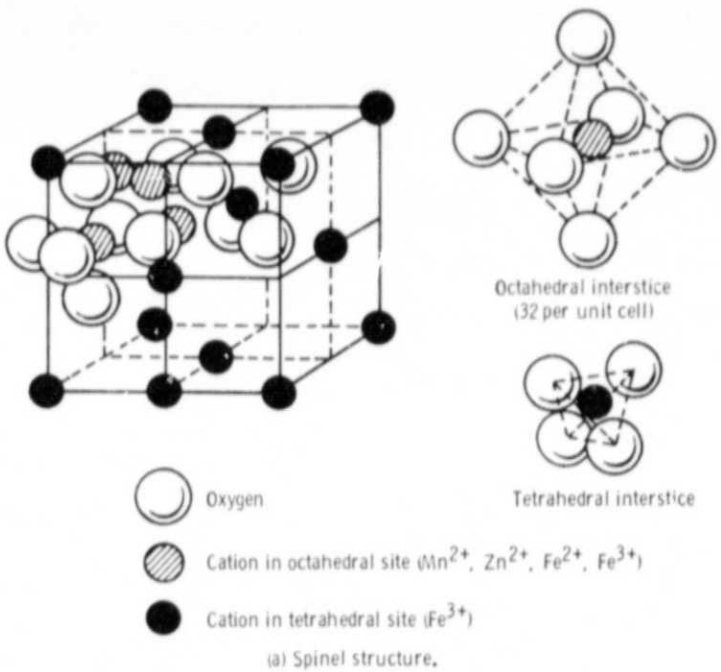

(a) Spinel structure.

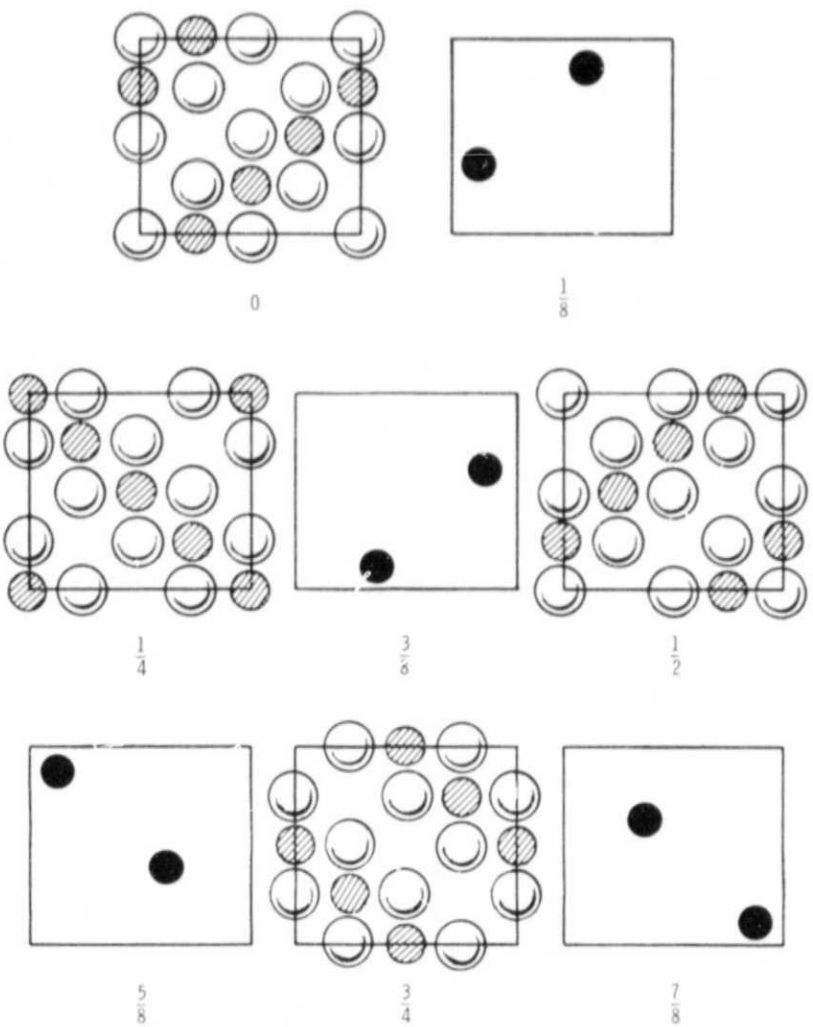

(b) Layers of atoms parallel to (100) plane.

Figure 1. - Spinel structure. (From refs. 1 and 2.)

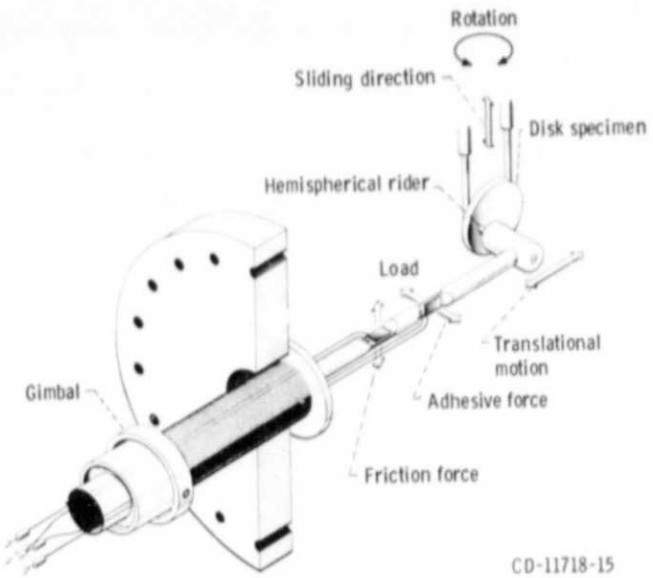

Figure 2. - High-vacuum friction-and-wear apparatus.

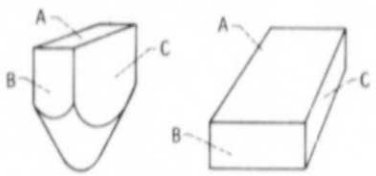

(a) Rider. (b) Disk.

Plane designation	Crystallographic plane			
A	(100)	(110)	(111)	(211)
B	(110)	(100)	(211)	(111)
C	(110)	(110)	(110)	(110)

Figure 3. - Orientation of single-crystal manganese-zinc ferrite riders and disks for sliding friction and wear tests in vacuum. ("A" plane parallel to sliding interface.)

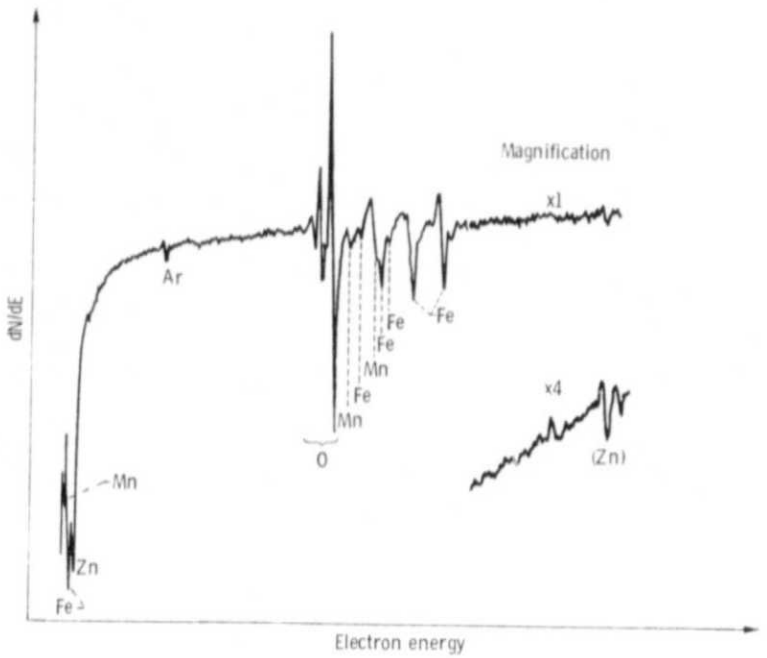

Figure 4. - Auger emission spectroscopy spectrum for manganese-zinc ferrite (110) surface after sputter cleaning.

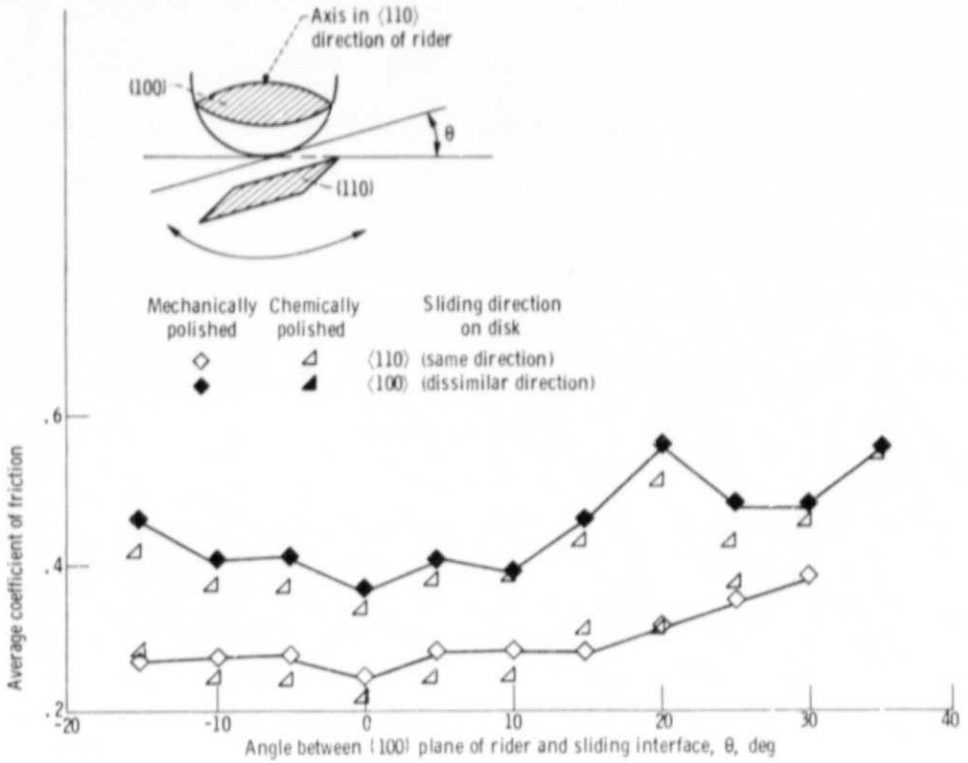

Figure 5. - Coefficients of friction for both mechanically polished and chemically etched surfaces of disks. Sliding direction of rider, ⟨100⟩; sliding directions on disk, ⟨110⟩ and ⟨100⟩; single pass sliding.

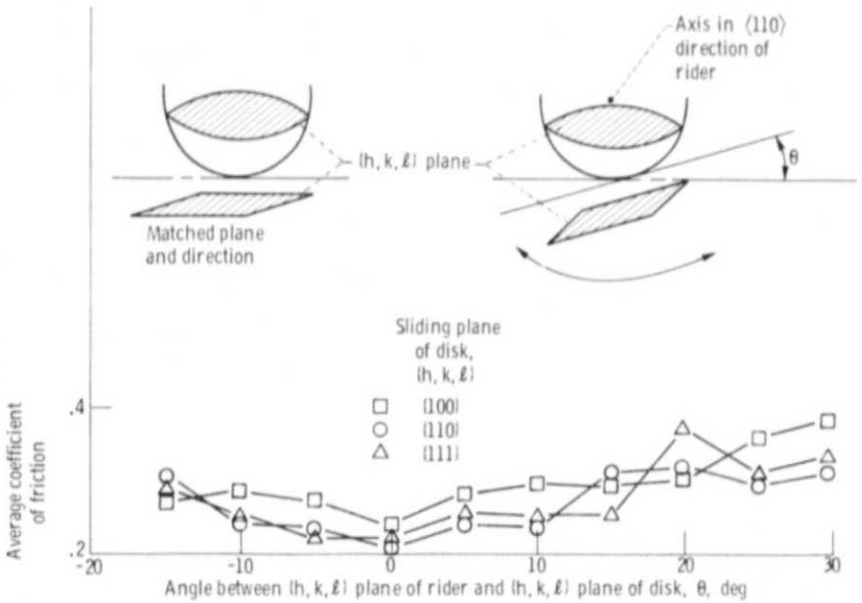

Figure 6. - Coefficient of friction as function of angle between (h, k, ℓ) plane of rider and (h, k, ℓ) plane of disk. Sliding direction for both riders and disks, ⟨110⟩; single pass; rider and disk material, manganese-zinc ferrite.

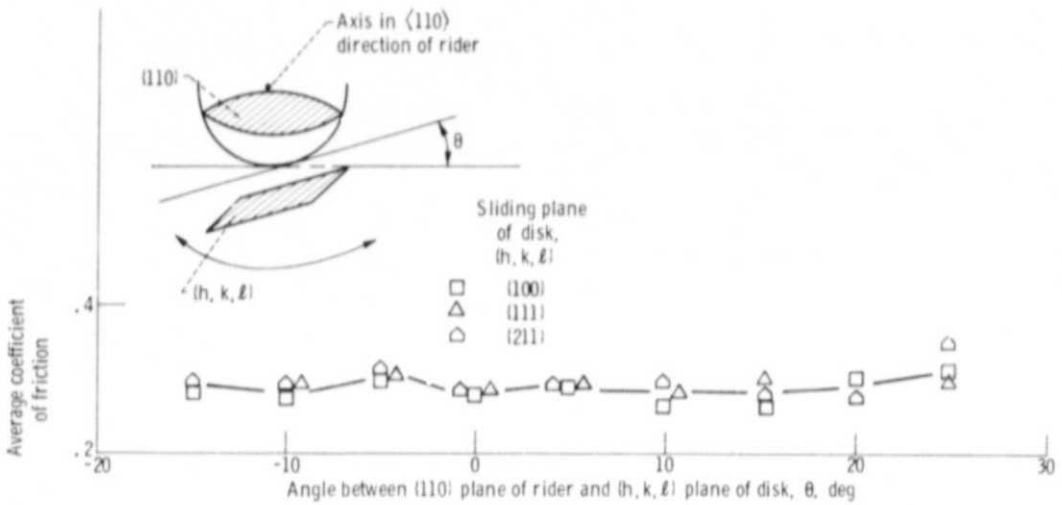

Figure 7. - Coefficient of friction as function of angle between {110} plane of rider and (h, k, ℓ) plane of disk. Sliding direction for both riders and disks, ⟨110⟩; single pass; rider and disk material, manganese-zinc ferrite.

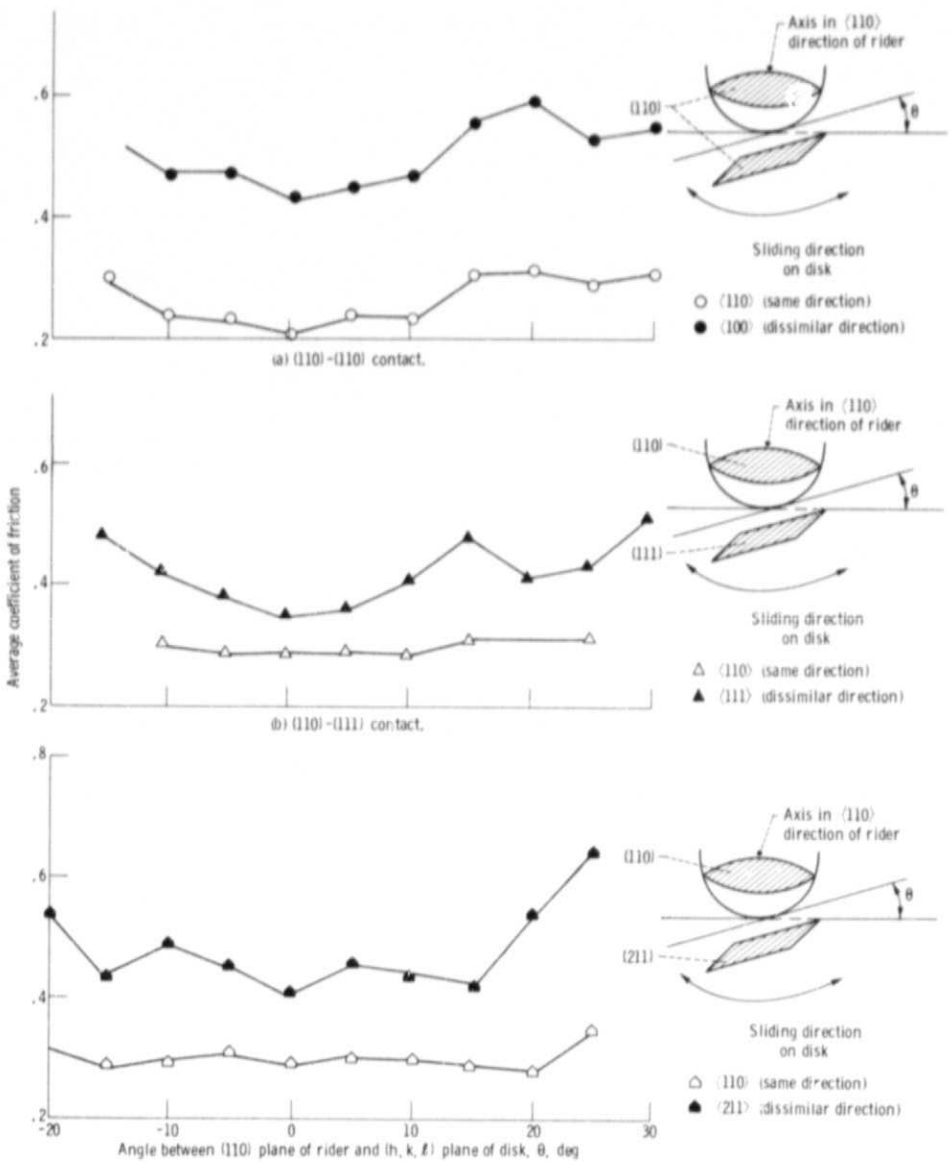

Figure 8. - Coefficients of friction for mating same and dissimilar directions of rider and disk. Sliding direction of rider, ⟨110⟩; single pass; rider and disk material, manganese-zinc ferrite.

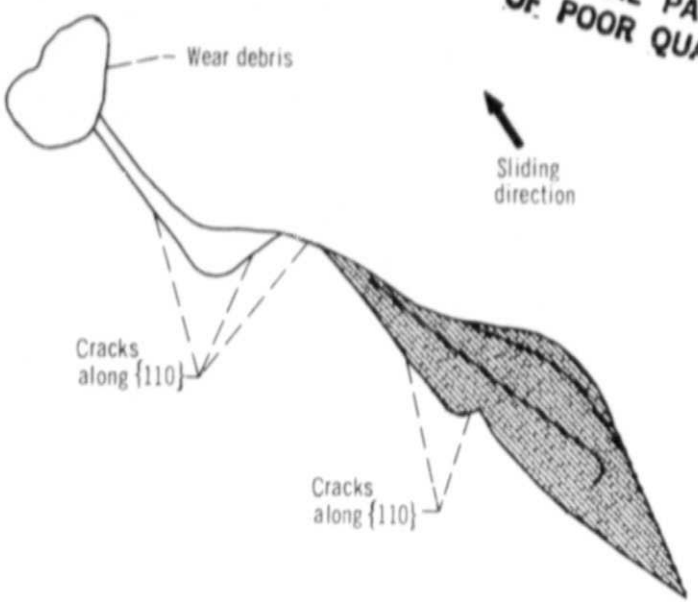

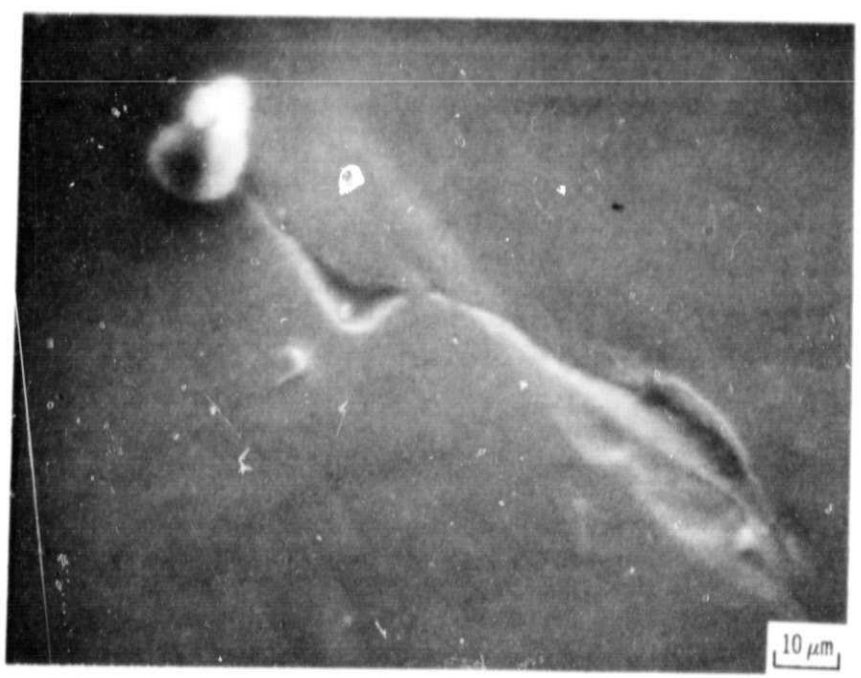

(a) Rider, with {110} plane parallel to interface.

Figure 9. - Scanning electron micrographs of cracking of single-crystal manganese-zinc ferrite {110} rider after 5 passes in sliding contact with single-crystal manganese-zinc ferrite {211} disk. Sliding direction for rider and disk, ⟨110⟩.

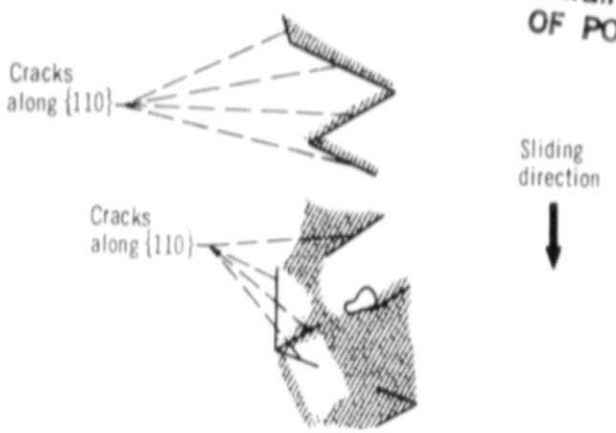

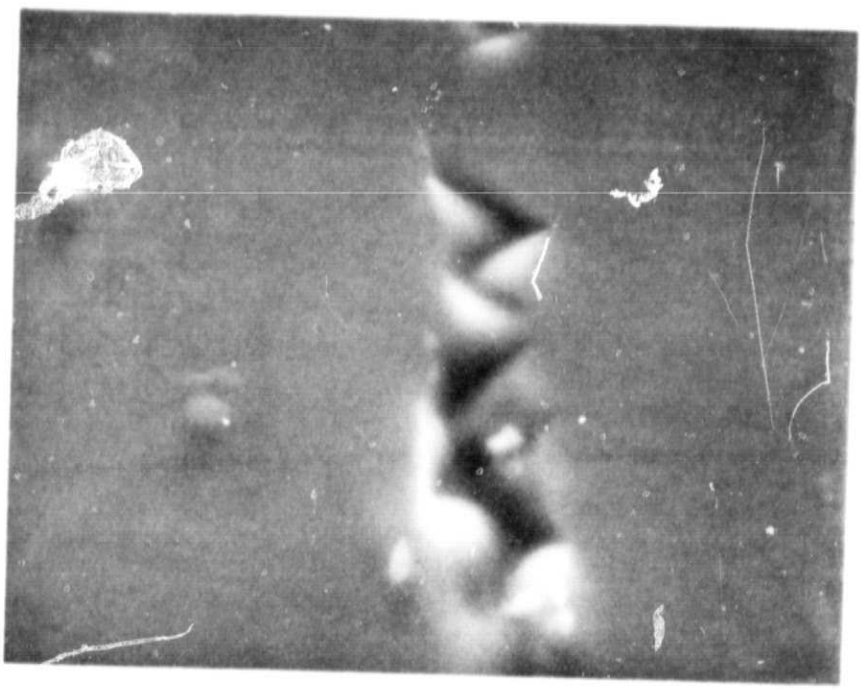

(b) Disk, with {211} plane parallel to interface.

Figure 9. - Concluded.

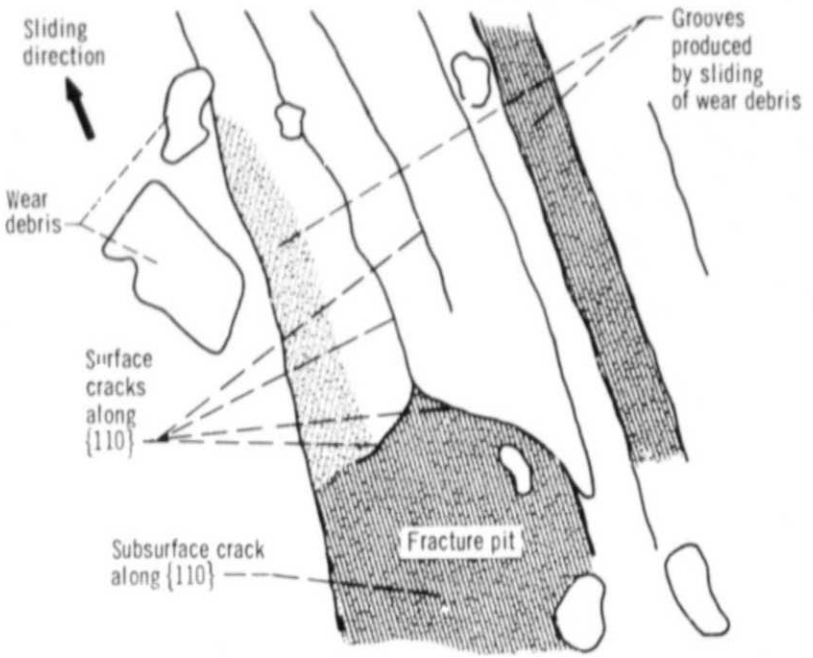

Figure 10. - Scanning electron micrograph of fracture pit and cracks on single-crystal manganese-zinc ferrite {110} rider after 20 passes in sliding contact with single-crystal manganese-zinc ferrite {110} disk. Sliding direction for rider and disk, ⟨110⟩.

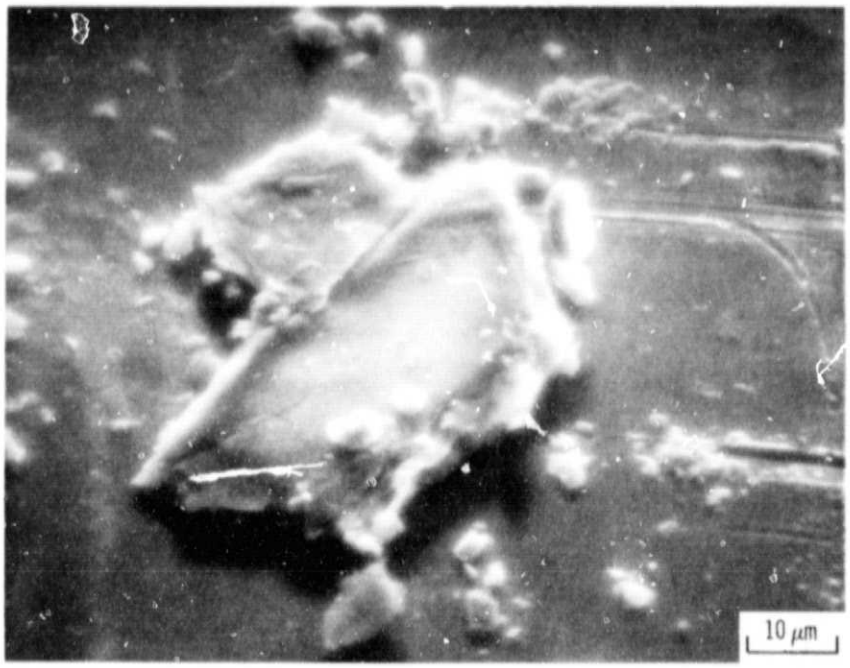

(a) Nearly completely hexagonal wear debris.

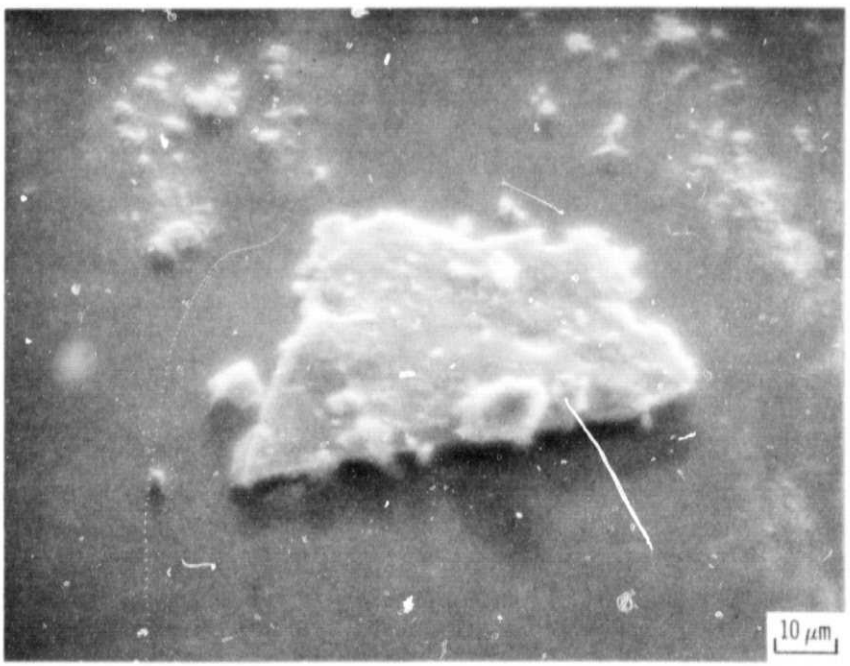

(b) Partially hexagonal wear debris.

Figure 11. - Scanning electron micrograph of wear track on single-crystal manganese-zinc ferrite {110} disk, showing transfer of hexagonal wear debris from single-crystal manganese-zinc ferrite {110} rider after 10 passes. Sliding direction for rider and disk, ⟨110⟩.

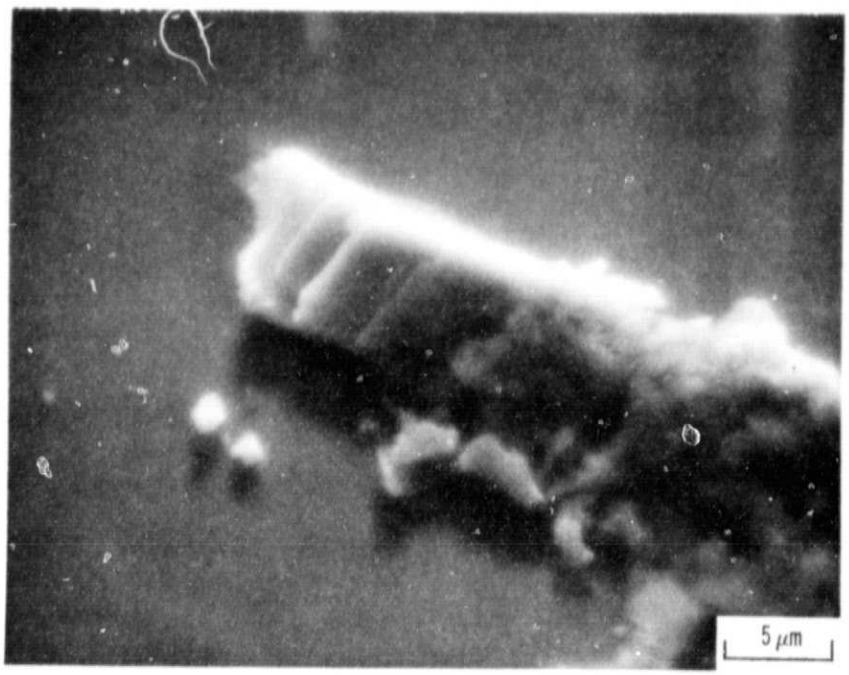

(c) Dislodged rectangular wear debris.

Figure 11. - Concluded.

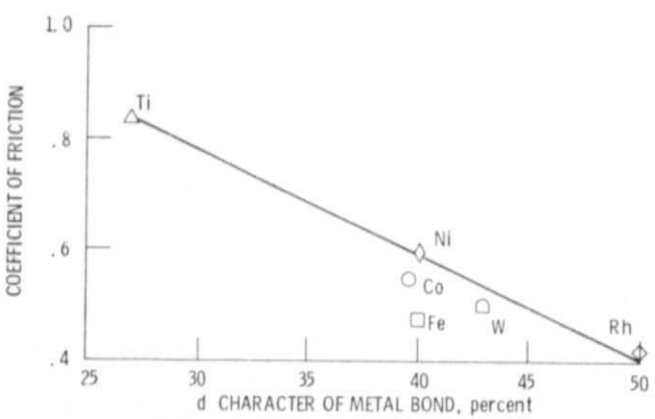

Figure 12. - Coefficient of friction as function of percent of d bond character of various metals in sliding contact with single-crystal manganese-zinc ferrite (110) surface in vacuum (10^{-8} N/m^2). Single pass; sliding velocity, 3 mm/min; load, 30 grams; temperature, 25° C.

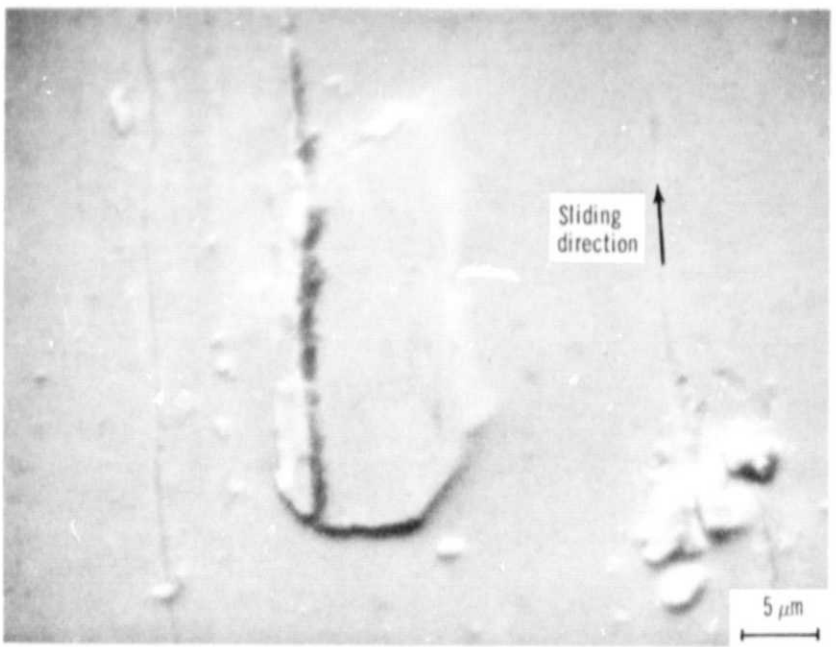

(a) Cracks propagating perpendicular to, parallel to, and at an inclination of about 45° to sliding direction.

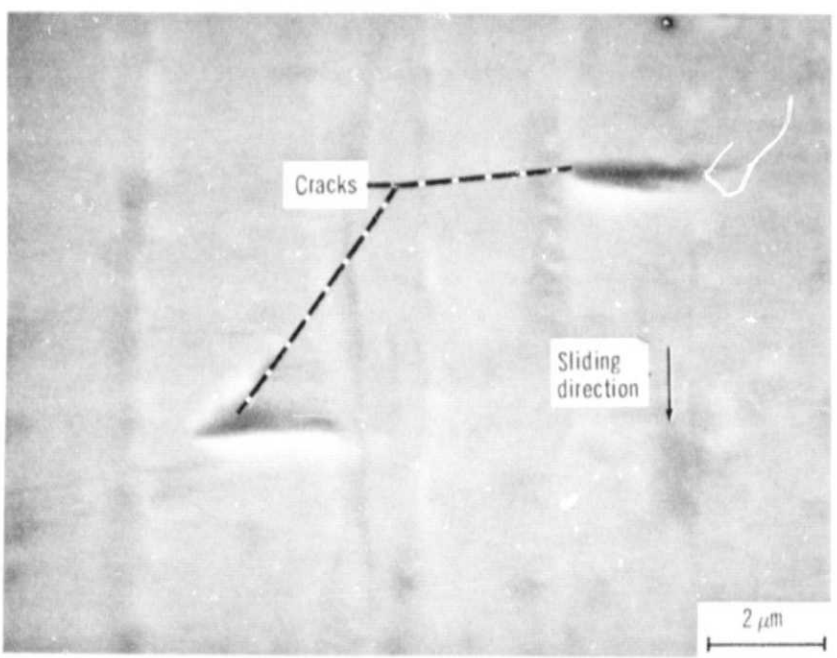

(b) Cracks propagating perpendicular to and at an inclination of 45° to sliding direction.

Figure 13. - Scanning electron micrographs of wear track and cracking of single-crystal manganese-zinc ferrite (110) surface after five passes of cobalt rider in high vacuum (10^{-8} N/m^2). Sliding velocity, 3 mm/min; temperature, 25° C.

(a) Wear debris.

(b) Manganese K_α X-ray map; $4.5X10^3$ counts.

Figure 14. - Scanning electron micrograph and energy dispersive X-ray analysis of wear debris of single-crystal manganese-zinc ferrite transferred to iron rider as result of five passes in high vacuum (10^{-8} N/m^2). Sliding velocity, 3 mm/min; temperature, 25° C.